Electronic Supplementary Material (ESI) for ChemComm.

Supporting Information for: Water Adsorption in UiO-66: The Importance of Defects

Pritha Ghosh, Yamil J. Colón, and Randall Q. Snurr

1 Simulation Details

Grand canonical Monte Carlo simulations were used to predict all adsorption isotherms. For water isotherms, 10^8 equilibration steps were run, after which 10^8 production steps were run. Such long simulations are needed to equilibrate adsorption of water. For CO_2 isotherms, 10^6 equilibrations steps were followed by the same number of production steps. Lennard-Jones parameters are shown in Table S1. A cutoff of 12.8 Å was used for Lennard-Jones interactions, leading to simulation boxes of 2x2x2 unit cells, along with analytical tail corrections. Lorentz-Berthelot mixing rules were used for all Lennard-Jones cross interactions. Framework charges were calculated using the REPEAT[1] method, exactly as detailed in our previous work on water isotherms,[2] and are provided in the attached structure files. Ewald summations were used.

For water isotherms, the absolute loading is reported, and for CO_2 isotherms the excess loading is reported.

Table S1 Lennard-Jones parameters for all atoms in this study

Atom Type	σ (Å)	ε / k_B (K)	q (e)	Force Field
C	3.473	47.856	Framework charge included in structure files	DREIDING[3]
O	3.033	48.158	Framework charge included in structure files	DREIDING
H	2.846	7.649	Framework charge included in structure files	DREIDING
Zr	2.783	34.7	Framework charge included in structure files	UFF[4]
O (TIP4P)	3.154	78	-	TIP4P[5]
H (TIP4P)	-	-	0.52	TIP4P
M (TIP4P)	-	-	-1.04	TIP4P
O (CO_2)	3.05	79	-0.35	TraPPE[6]
C (CO_2)	2.80	27	0.7	TraPPE

2 Pore Size Distributions and Nitrogen Isotherms of all 3 Unit Cells

Pore size distributions were calculated using Poreblazer, version 3.0.2.[7]

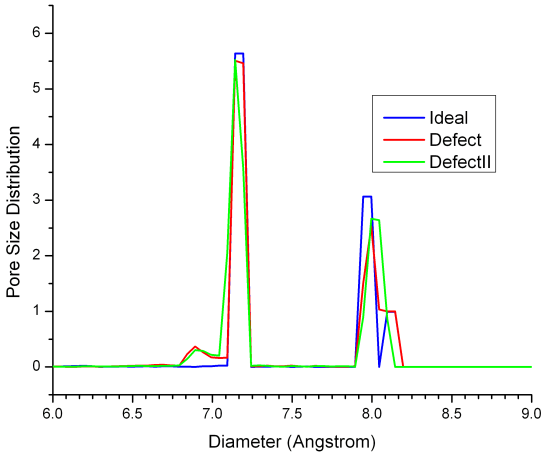

Fig. S1 Geometric pore size distribution for each of the structures considered

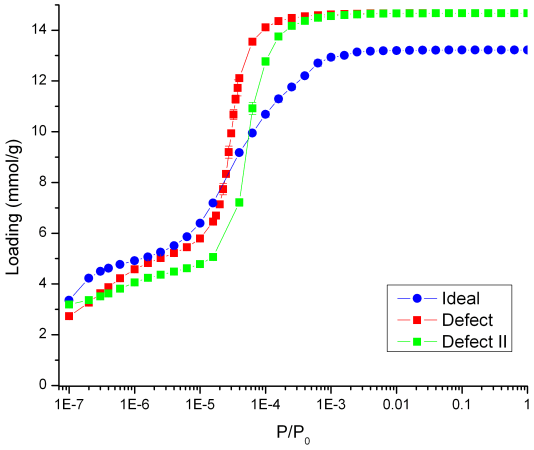

Fig. S2 Simulated nitrogen isotherms for the ideal and defect UiO-66 unit cells at 77 K

3 BET Surface Area Plots for Ideal and Defect Unit Cells

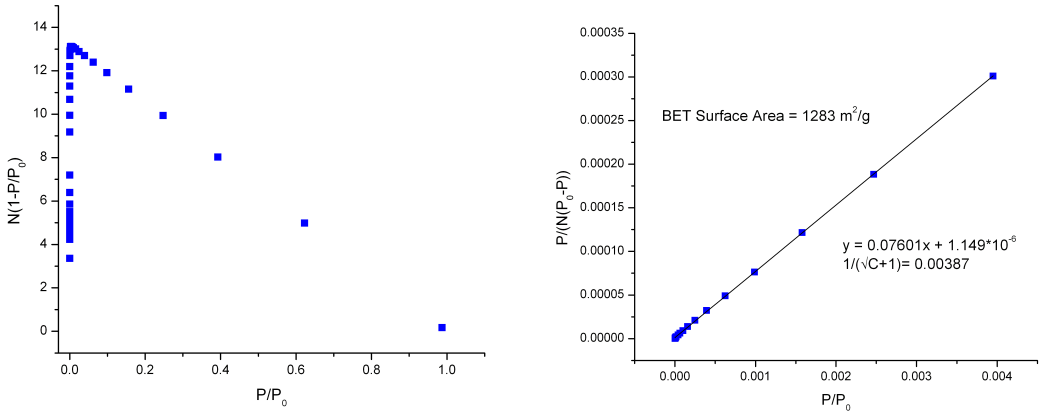

Fig. S3 BET surface area calculation for ideal UiO-66 from simulated nitrogen isotherm at 77 K. Graph on the left was to determine maximum P/P_0 to fulfill first consistency criterion. Graph on the right shows the linear regression on selected P/P_0 range, fulfilling second consistency criterion, and resulting BET surface area. It also shows the $1/(\sqrt{C}+1)$ value, which lies within the selected P/P_0 range, fulfilling the third consistency criterion.

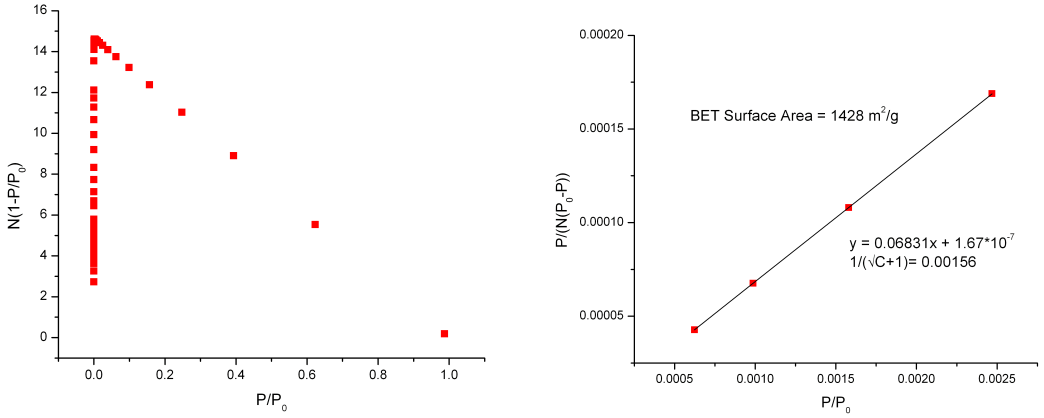

Fig. S4 BET surface area calculation for defect UiO-66 from simulated nitrogen isotherm at 77 K. Graph on the left was to determine maximum P/P_0 to fulfill first consistency criterion. Graph on the right shows the linear regression on selected P/P_0 range, fulfilling second consistency criterion, and resulting BET surface area. It also shows the $1/(\sqrt{C}+1)$ value, which lies within the selected P/P_0 range, fulfilling the third consistency criterion.

4 Adsorption and Desorption Isotherms for Ideal UiO-66

Desorption isotherms are run in the same fashion as adsorption isotherms, with the only difference being the starting configuration of the simulation box. In adsorption isotherms, the simulation box initially contains only the framework atoms with no adsorbates. In desorption isotherms, the initial simulation box is the framework saturated with adsorbate molecules. In this case, the starting configuration for every point on the desorption isotherm was the equilibrated configuration from $P/P_0 = 1$ from the adsorption isotherm.

P_0 in all water simulations in this work is considered to be 4.1 kPa, which is the vapor pressure of TIP4P water.[8]

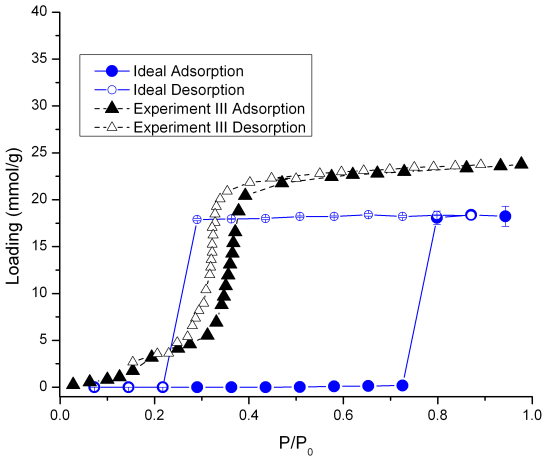

Fig. S5 Simulated water adsorption (closed circles) and desorption (open circles) for ideal UiO-66 at 298 K

5 Heats of Adsorption for CO_2 in Ideal and Defective Unit Cells

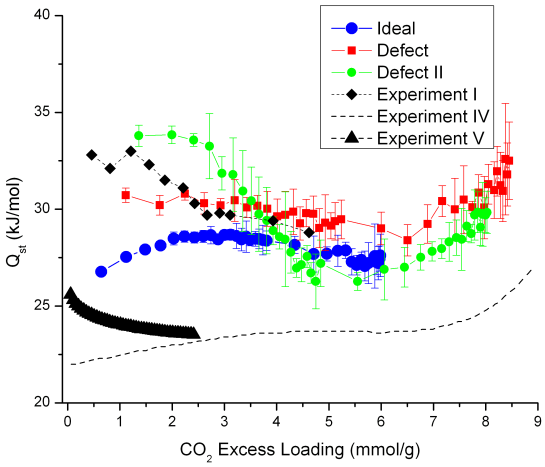

Fig. S6 Heats of adsorption for CO_2 at 300 K - comparison between simulated (ideal and two defect unit cells) and experiments I[9], IV[10], and V[11]

References

1 C. Campañá, B. Mussard and T. K. Woo, *Journal of Chemical Theory and Computation*, 2009, **5**, 2866–2878.
2 P. Ghosh, K. C. Kim and R. Q. Snurr, *The Journal of Physical Chemistry C*, 2014, **118**, 1102–1110.
3 S. L. Mayo, B. D. Olafson and W. A. Goddard III, *Journal of Physical Chemistry*, 1990, **94**, 8897–8909.
4 A. K. Rappe, C. J. Casewit, K. S. Colwell, W. A. Goddard III and W. M. Skiff, *Journal of the American Chemical Society*, 1992, **114**, 10024–10035.
5 W. L. Jorgensen, J. Chandrasekhar, J. D. Madura, R. W. Impey and M. L. Klein, *The Journal of Chemical Physics*, 1983, **79**, 926–935.
6 J. J. Potoff and J. I. Siepmann, *AIChE Journal*, 2001, **47**, 1676–1682.
7 L. Sarkisov and A. Harrison, *Molecular Simulation*, 2011, **37**, 1248–1257.
8 C. Vega, J. L. F. Abascal and I. Nezbeda, *The Journal of Chemical Physics*, 2006, **125**, 34503.
9 A. D. Wiersum, E. Soubeyrand-Lenoir, Q. Yang, B. Moulin, V. Guillerm, M. B. Yahia, S. Bourrelly, A. Vimont, S. Miller, C. Vagner, M. Daturi, G. Clet, C. Serre, G. Maurin and P. L. Llewellyn, *Chemistry, an Asian Journal*, 2011, **6**, 3270–80.
10 H. Wu, Y. S. Chua, V. Krungleviciute, M. Tyagi, P. Chen, T. Yildirim and W. Zhou, *Journal of the American Chemical Society*, 2013, **135**, 10525–32.
11 G. E. Cmarik, M. Kim, S. M. Cohen and K. S. Walton, *Langmuir*, 2012, **28**, 15606–13.